ELSEVIER

Airborne particulate organics at the summit (2060 m, a.s.l.) of Mt. Hua in central China during winter: Implications for biofuel and coal combustion

Jianjun Li [a,b], Gehui Wang [a,c,*], Bianhong Zhou [d], Chunlei Cheng [a], Junji Cao [a,c], Zhenxing Shen [b,a], Zhisheng An [a]

[a] State Key Laboratory of Loess and Quaternary Geology, Institute of Earth Environment, Chinese Academy of Sciences, Xi'an 710075, China
[b] Department of Environmental Science and Engineering, Xi'an Jiaotong University, Xi'an 710049, China
[c] School of Human Settlements and Civil Engineering, Xi'an Jiaotong University, Xi'an 710049, China
[d] Department of Geographical Science and Environment Engineering, Baoji University of Art and Science, Baoji 721013, China

ARTICLE INFO

ABSTRACT

Sugars, n-alkanes and PAHs in PM_{10} and size-segregated samples collected from the summit (2060 m, altitude) of Mt. Hua in Guanzhong Plain, central China during the winter of 2009 were characterized using a GC/MS technique. Concentrations of sugars, n-alkanes and PAHs in PM_{10} are 107 ± 52, 121 ± 63, 7.3 ± 3.4 ng m^{-3}, respectively. Levoglucosan and fossil fuel derived n-alkanes are more abundant in the air masses transported from southern China than in those from northern China with no spatial difference found for PAHs, suggesting that emissions from biomass burning and vehicle exhausts are more significant in southern part of the country. Dehydrated sugars, fossil fuel derived n-alkanes and PAHs presented a unimode size distribution, peaking at the size of 0.7–1.1 μm, whereas non-dehydrated sugars and plant wax derived n-alkanes showed a bimodal pattern, peaking at 0.7–2.1 and 5.8–9.0 μm, respectively.
Principal component analysis showed that biofuel combustion plus plant emission is the most important source in Mt. Hua, being different from the cases in Chinese urban areas where fossil fuel combustion is the major source. By comparison with previous mountain and lowland observations and aircraft measurements we found that wintertime PAHs in China are still characterized by coal burning emissions especially in the inland regions, although in the country increasing rate of SO_2 emission from coal combustion has decreased and emissions of vehicle exhaust has sharply increased.

1. Introduction

No other region on Earth is as large and diverse a source of aerosols and trace gases as the Asian continent, especially in East Asia, where much more absorbing soot and carbonaceous aerosols have been emitted into the atmosphere. Those anthropogenic aerosols may result in heavily polluted clouds and evaporate much of their water before precipitation can occur. Rosenfeld et al. (2007) reported that in the past 50 years increasing aerosols in central China have resulted in a decreasing rainfall. Menon et al. (2002) also pointed out that high loading of carbonaceous aerosols (e.g., black carbon) in China is one of major factors leading to the increased floods in the south and droughts in the north. Coal is the major energy source in China, and more than 2 billion tons of coal are burned each year without a strict emission control in some cases, especially in winter when coals are combusted for heating (Huebert et al., 2003; Wang et al., 2006, 2009a). In addition, biomass burning for cooking and heating is still common in rural area of China, adding additional carbonaceous particles into the atmosphere.

* Corresponding author at: State Key Laboratory of Loess and Quaternary Geology, Institute of Earth Environment, Chinese Academy of Sciences, Xi'an 710075, China. Tel.: +86 29 8832 9320; fax: +86 29 8832 0456.
E-mail addresses: wanggh@ieecas.cn, gehuiwang@yahoo.com.cn (G. Wang).

A five-year satellite observation suggests that North China Plain, Guanzhong Plain, and Sichuan Basin in China are the three most heavily polluted regions in the world, where averaged annual $PM_{2.5}$ on the ground surface are more than $80\ \mu g\ m^{-3}$ (van Donkelaar et al., 2010). Being different from North China Plain and Sichuan Basin, Guanzhong Plain is a semi-arid region, where economic development level is relatively lower. Therefore influence of anthropogenic pollutants on the air quality is expected to be different from that in economically developed regions like North China Plain. Mountain area is a receptor for anthropogenic aerosols originating from lowlands by long-range transport, and thus characterizations of alpine organic aerosols can improve our understanding the impact of anthropogenic activities on a large-scale of atmospheric environment. Organic aerosols in Chinese mega-cities have been given much attention, but characteristics of organic aerosols from Guanzhong Plain were documented in a limited number (Wang et al., 2010; Xie et al., 2009, 2010) with no report for those in the atmosphere over alpine regions. An aerosol sampling campaign was performed during the winter of 2008 at Mt. Hua in Guanzhong Plain, central China to investigate the properties of air pollution in the region. Here we first characterized the molecular composition and size distributions of organic aerosols in the Mt. Hua atmosphere, and then compared the observation with those conducting at lowland sites to identify the characters of air pollution over the mountain region.

2. Experiment

2.1. Sampling

PM_{10} and size-segregated samples were simultaneously collected at the summit (34°29′ N, 110°05′E, 2060 m a.s.l., Fig. 1) of Mt. Hua during Jan. 11–22, 2009, which is a typical time of burning biofuel and coal for house heating in

Guanzhong Plain. A medium-volume air sampler (KC-120H, made in China) for PM_{10} was operated at an airflow rate of $100\ L\ min^{-1}$. Size-segregated aerosol samples were collected using an Andersen 9-stage air sampler (Thermo electronic Company, USA) with the cutoff points at 9.0, 5.8, 4.7, 3.3, 2.1, 1.1, 0.7, and 0.4 μm under an airflow rate of $28.3\ L\ min^{-1}$. 21 PM_{10} samples (10 in the day and 11 at night) were collected on a day/night basis each for 10 hr, and 3 sets of the size-resolved aerosol samples (9 samples per set) were collected with a 4-day duration in each. All samples were collected onto pre-baked (450 °C for 8 h) quartz microfiber filters (Whatman 42). After sampling, the filter was sealed in an aluminum bag and stored at −18 °C prior to analysis. Field blank samples were collected before and after sampling by mounting the filters onto the sampler for about 10 min without sucking any air. Meteorological parameters were hourly monitored during the campaign and summarized in Table 1.

2.2. Extraction and derivatization

Detailed methods for extraction, derivatization and gas chromatography/mass spectrometry (GC/MS) analysis were described elsewhere (Wang et al., 2009b, 2009c). Briefly, one fourth of the sample/blank filter was cut in pieces and extracted with a mixture of dichloromethane and methanol (2:1, v/v) under ultrasonication. The extracts were concentrated using a rotary evaporator under a vacuum condition and then blown down to dryness using a pure nitrogen stream. After reaction with N,O-bis-(trimethylsilyl) trifluoroacetamide (BSTFA) at 70 °C for 3 h, the derivatives were determined using a GC/MS technique below.

2.3. Gas chromatography−mass spectrometry

Gas chromatography− mass spectrometry (GC/MS) analysis of the derivatized fraction was performed using an Agilent
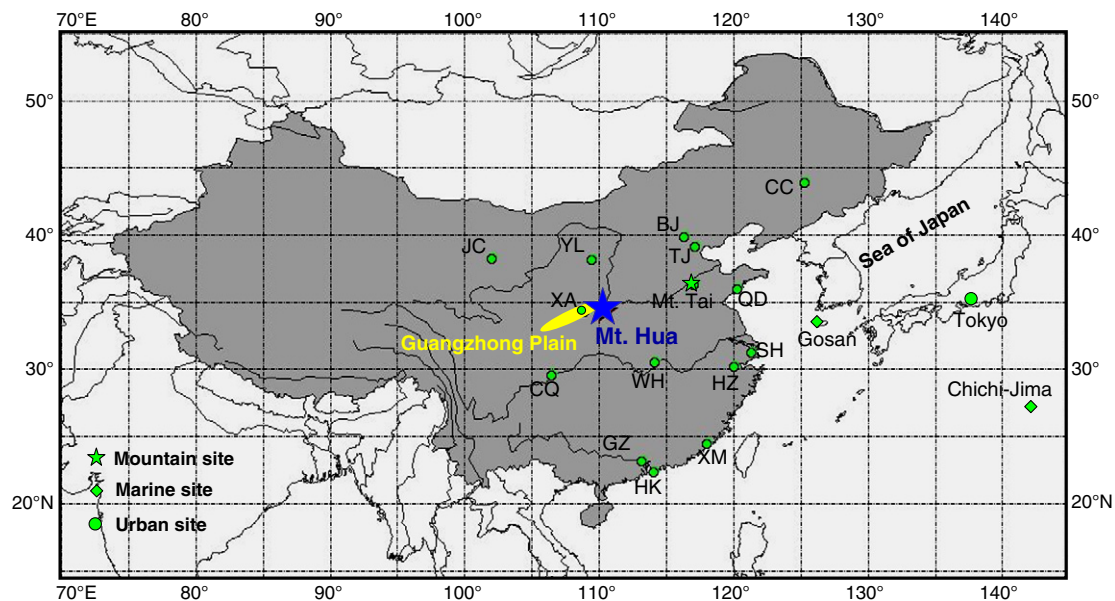

Fig. 1. Locations of the sampling site (Mt. Hua) and other mountain, marine and urban regions. City code: HK (Hong Kong), GZ (Guangzhou), XM (Xiamen), CQ (Chongqing), HZ (Hangzhou), WH (Wuhan), SH (Shanghai), XA (Xi'an), QD (Qingdao), YL (Yulin), JC (Jinchang), TJ (Tianjin), BJ (Beijing) and CC (Changchun).

Table 1
Meteorological data during the Mt. Hua sampling period[a].

	Daytime 0700–1800 Local Time			Nighttime 1900–0600 Local Time		
	Max	Min	Ave ± SD	Max	Min	Ave ± SD
Temperature, °C	−13	1.3	−2.8 ± 3.8	−14	1.4	−4.4 ± 4.2
Relative humidity, %	10	96	38 ± 26	24	90	38 ± 18
Wind direction, deg	208	292	256 ± 25	221	309	272 ± 32
Wind speed, m s^{-1}	1.6	8.9	4.9 ± 2	3.7	10.6	6.9 ± 2.2
Pressure, hPa	790	803	797 ± 4	787	803	797 ± 4
Visibility, km	27	12	20 ± 4	26	14	20 ± 3

[a] Sampling period is 11–22 Jan. 2009. All the meteorological parameters were measured hourly.

7890A GC coupled with an Agilent 5975 C MSD. The GC separation was carried out on a HP-5MS fused silica capillary column with the GC oven temperature programmed from 50 °C (2 min) to 120 °C at 15 °C min^{-1} and then to 300 °C at 5 °C min^{-1} with a final isothermal hold at 300 °C for 16 min. The sample was injected in a splitless mode at an injector temperature of 280 °C, and scanned from 50 to 650 Daltons using electron impact (EI) mode at 70 eV. GC/MS response factors were determined using authentic standards. Method detection limits (MDLs) for major compounds, i.e., levoglucosan (Levo) , sucrose (Sucr), nonacosane (C_{29}), hentriacotane (C_{31}), benzo (b/k)fluoranthene (BbkF) and indeno[123-cd]pyrene (IP) were 0.17, 0.02, 0.04, 0.09, 0.01 and 0.01 ng m^{-3}, respectively. Recoveries of the target compounds were better than 85%. No target compound was found in the blanks. Data presented here were corrected for the field blanks but not corrected for the recoveries. Similar to inorganic ions (Li et al., 2011), a strong linear correlation was obtained for the major organic compounds in the PM_{10} samples and in the summed size fractions (PM_9) of the size-segregated samples (Fig. 2),demonstrating a good consistency between the two data sets. However, concentrations obtained by the size-resolved sampler are nearly 20% higher than those measured by the PM_{10} sampler, which was most likely resulted from the loss of evaporation owing to the pressure drop in PM_{10} sampler (Peters and Seifert, 1980; McMurry, 2000; Wang et al., 2009a). Organic
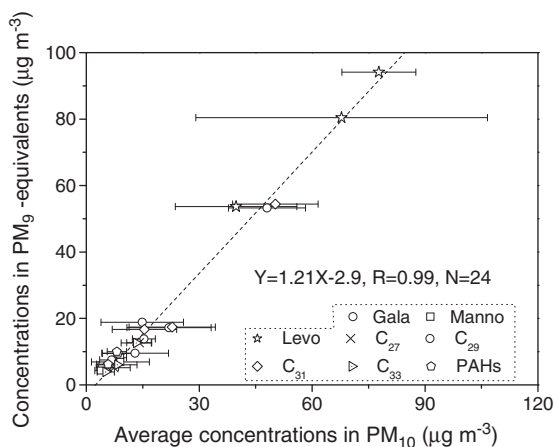
Fig. 2. An intercomparison of concentrations of major organic compounds determined in the PM_{10} samples (collected by KC-120H sampler) and in the PM_9-equivalent fraction of the size-segregated samples (the sum of the compounds in the stages of <0.4, 0.4–0.7, 0.7–1.1, 1.1–2.1, 2.1–3.3, 3.3–4.7, 4.7–5.8 and 5.8–9.0 μm collected by Andersen 9-stage air sampler).

carbon (OC), elemental carbon (EC) and inorganic ions have been reported elsewhere (Li et al., 2011) and cited here to investigate the mountain aerosol characters.

3. Results and discussion

3.1. Concentrations and molecular compositions of sugars, n-alkanes and PAHs in PM_{10}

3.1.1. Sugars

Levoglucosan (65 ± 30 ng m^{-3}), a key tracer for combustion of cellulose (Engling et al., 2009; Oros et al., 2006; Simoneit et al., 1999), was found to be the most abundant component in the sugar class (Table 2), followed by galactosan (12 ± 6.8 ng m^{-3}) and mannosan (7.8 ± 5.4 ng m^{-3}), another two tracers of biomass burning emissions (Pio et al., 2008; Wang et al., 2009d). Levoglucosan showed a robust linear correlation with galactosan (R = 0.97) and mannosan (R = 0.94) (Fig. 3a), suggesting that they may commonly be produced from biofuel combustion in the region. Major fraction of airborne potassium ion (K^+) originates from biomass burning emissions (Andreae et al., 1990), although a minor amount can be derived from soil dust (Shen et al., 2008; Wang et al., 2009a). It is thus plausible that K^+ in the PM_{10} samples well correlated with the three dehydrated sugars (Fig. 3b), further indicating the significant influence of biomass burning emission on the alpine aerosols. In addition, inositol might also be originated from biomass burning as it well correlated with galactosan, mannosan and levoglucosan (Fig. 3c). Non-dehydrated saccharides including monosaccharides (i.e., glucose and fructose), disaccharides (i.e., sucrose and trehalose) and sugar polyols (i.e., arabitol and mannitol) are the major forms of photosynthetically assimilated carbon in the biosphere, and their sources include soil microbiota, plants and animals (Simoneit et al., 2004a; Medeiros et al., 2006). Concentrations of these compounds except sucrose strongly correlated one another (Table 3), indicating an importance of biogenic sources. These non-dehydrated sugars also presented a higher concentration in daytime than in nighttime due to enhanced biogenic activities.

3.1.2. n-Alkanes

Total *n*-alkanes of PM_{10} at Mt. Hua are 119 ± 61 ng m^{-3} in daytime and 122 ± 65 ng m^{-3} in nighttime with no significant diurnal differences (Table 2). Unlike the cases in urban and rural areas where aerosol concentration generally increases at night due to the planetary boundary layer (PBL) shrink, Mt. Hua site is 1500 m above the ground and probably

Table 2
Concentrations of sugars, n-alkanes and PAHs in PM_{10} from Mt. Hua during winter, ng m^{-3}.

	Day (N = 10)	Night (N = 11)	Daily average (N = 21)
I. Sugars			
Galactosan (Gala)	13 ± 6.3	12 ± 7.3	12 ± 6.8
Mannosan (Manno)	8.2 ± 5.2	7.4 ± 5.6	7.8 ± 5.4
Levoglucosan (Levo)	65 ± 30	65 ± 30	65 ± 30
Arabitol (Arab)	3.1 ± 2.2	2.8 ± 1.8	3.0 ± 2.0
Fructose (Fluc)	6.3 ± 6.2	4.5 ± 3.3	5.4 ± 5.0
Glucose (Gluc)	6.2 ± 5.4	4.8 ± 3.6	5.5 ± 4.6
Mannitol (Manni)	2.4 ± 2.2	1.9 ± 1.3	2.2 ± 1.8
Inositol (Inos)	0.3 ± 0.3	0.3 ± 0.3	0.3 ± 0.3
Sucrose (Sucr)	3.1 ± 2.4	2.6 ± 2.7	2.8 ± 2.6
Trehalose (Treh)	2.8 ± 2.5	2.3 ± 1.9	2.5 ± 2.2
Subtotal	110 ± 53	104 ± 51	107 ± 52
Total sugars-C/OC (%)	0.79 ± 0.20	0.75 ± 0.12	0.77 ± 0.17
II. n-Alkanes			
Octadecane (C_{18})	1.3 ± 0.3	1.2 ± 0.3	1.2 ± 0.3
Nonadecane (C_{19})	1.1 ± 0.3	0.8 ± 0.2	0.9 ± 0.3
Icosane (C_{20})	1.0 ± 0.3	0.9 ± 0.3	1.0 ± 0.3
Henicosane (C_{21})	1.7 ± 0.8	1.7 ± 0.8	1.7 ± 0.8
Docosane (C_{22})	2.0 ± 1.1	2.2 ± 1.1	2.1 ± 1.1
Tricosane (C_{23})	3.4 ± 1.9	3.8 ± 1.8	3.6 ± 1.9
Tetracosane (C_{24})	3.0 ± 1.6	3.3 ± 1.7	3.1 ± 1.6
Pentacosane (C_{25})	4.8 ± 2.4	5.1 ± 2.5	5.0 ± 2.5
Hexacosane (C_{26})	3.3 ± 1.6	3.5 ± 1.6	3.4 ± 1.6
Heptacosane (C_{27})	9.1 ± 4.8	9.9 ± 5.4	9.5 ± 5.6
Octacosane (C_{28})	4.8 ± 2.4	4.9 ± 2.4	4.8 ± 2.4
Nonacosane (C_{29})	29 ± 17	31 ± 19	30 ± 18
Triacotane (C_{30})	4.8 ± 2.7	4.9 ± 2.5	4.9 ± 2.6
Hentriacotane (C_{31})	32 ± 18	31 ± 19	32 ± 18
Dotriacotane (C_{32})	3.5 ± 2.2	3.6 ± 2.0	3.5 ± 2.1
Tritriacotane (C_{33})	9.5 ± 5.1	9.4 ± 5.5	9.4 ± 5.3
Tetratriacotane (C_{34})	2.2 ± 1.6	2.3 ± 1.5	2.2 ± 1.6
Pentatriacotane (C_{35})	3.0 ± 2.4	2.6 ± 1.6	2.8 ± 2.1
Subtotal	119 ± 61	122 ± 65	121 ± 63
Plant wax[a]	68 ± 40	70 ± 42	69 ± 41
Fossil fuel[a]	52 ± 25	53 ± 25	52 ± 25
Total n-alkane-C/OC (%)	1.6 ± 0.6	1.8 ± 0.7	1.7 ± 0.7
III. PAHs			
Phenanthrene (Phe)	0.9 ± 0.3	0.9 ± 0.3	0.9 ± 0.3
Anthracene (Ant)	0.2 ± 0.1	0.2 ± 0.1	0.2 ± 0.1
Fluoranthene (Flu)	1.1 ± 0.4	1.0 ± 0.4	1.1 ± 0.4
Pyrene (Pyr)	0.5 ± 0.2	0.6 ± 0.3	0.6 ± 0.3
216 PAH isomers	0.4 ± 0.2	0.4 ± 0.3	0.4 ± 0.2
Benz(a)anthracene (BaA)	0.2 ± 0.1	0.3 ± 0.2	0.3 ± 0.2
Chrysene/Triphenylene (CT)	0.6 ± 0.3	0.6 ± 0.3	0.6 ± 0.3
Benzo(b/k)fluoranthene (BbkF)	0.9 ± 0.5	1.0 ± 0.5	0.9 ± 0.5
Benzo(e)pyrene (BeP)	0.7 ± 0.5	0.8 ± 0.5	0.8 ± 0.5
Benzo(a)pyrene (BaP)	0.4 ± 0.2	0.4 ± 0.2	0.4 ± 0.2
Perylene (Per)	0.1 ± 0.0	0.1 ± 0.0	0.1 ± 0.0
Indeno[123-cd]pyrene (IP)	0.6 ± 0.3	0.7 ± 0.4	0.7 ± 0.4
Dibenz(a,h)anthracene (DBA)	0.1 ± 0.1	0.1 ± 0.1	0.1 ± 0.1
Benzo(ghi)perylene (BghiP)	0.2 ± 0.1	0.3 ± 0.2	0.3 ± 0.2
Coronene (Cor)	0.2 ± 0.1	0.2 ± 0.1	0.2 ± 0.1
Subtotal	7.0 ± 3.0	7.6 ± 3.7	7.3 ± 3.4
Total PAHs-C/OC (%)	0.12 ± 0.07	0.14 ± 0.09	0.13 ± 0.08
PM_{10} (µg m^{-3})	51 ± 25	56 ± 26	54 ± 24
OC (µg m^{-3})	6.0 ± 2.2	5.9 ± 2.7	5.9 ± 2.5
EC (µg m^{-3})	0.8 ± 0.4	0.9 ± 0.5	0.9 ± 0.5

[a] Plant wax n-alkanes: calculated as the excess odd homologues-adjacent even homologues average and the difference from the total nalkanes is the fossil fuel-derived amount (Simoneit et al., 1991, 2004b).

isolated from the PBL especially in winter. Therefore, n-alkanes in the samples are affected mostly by regional sources rather than local ones, resulting in no clear diurnal

variations. Molecular distributions of the alpine n-alkanes showed a major peak at C_{29} or C_{31}. n-Alkanes derived from plant wax are dominated by high molecular weight species (HMW, carbon number >25) with an odd number preference. However, fossil fuel derived n-alkanes generally present no odd/even number preference (Ladji et al., 2009; Rogge et al., 1993; Simoneit et al., 2004b). In the Mt. Hua samples HMW n-alkanes accounted for about 85% of the total with plant wax derived n-alkanes being 69 ± 41 ng m^{-3} and fossil fuel derived n-alkanes being 52 ± 25 ng m^{-3}, suggesting that natural plant emission is a major source of the normal alkanes at Mt. Hua, which is different from the cases in lowland areas of Guanzhong Plain, where more than 70% of n-alkanes are derived from fossil fuel combustion (Wang et al., 2006; Xie et al., 2009).

3.1.3. PAHs

Similarly, no clear diurnal difference was found for total PAHs in PM_{10} samples (7.0 ± 3.0 ng m^{-3} in daytime and 7.6 ± 3.7 ng m^{-3} in nighttime, Table 2), further indicating that PAHs in the mountain air are largely derived from regional sources. The most abundant PAH is fluoranthene (Flu), whose day- and night- time concentrations are separately 1.1 ± 0.4 and 1.0 ± 0.4 ng m^{-3} (Table 2), followed by benzo(b/k)fluoranthene (BbkF) and phenanthrene (Phe). Compared to those in urban areas (Wang et al., 2006; Xie et al., 2010), low molecular weight (LMW) Phe and Flu are more abundant in the Mt. Hua air, which is attributable to an increased transformation of the gaseous species to the solid phase due to lower temperature of the mountaintop atmosphere (Gaga and Ari, 2011; Hanedar et al., 2011). As shown in Fig. 3d, PAHs presented good linear correlations with EC and F$^-$, because they all mostly originate from fossil fuel combustion (Li et al., 2011; Xie et al., 2009 and 2010). In our previous study on PM_{10} in Baoji, a mid-scale city nearby Mt. Hua, we found a good correlation between PAHs and sulfate, both are largely derived from coal combustion (Wang et al., 2010). However, such a correlation was not observed for the Mt. Hua samples (R = 0.30), which can be ascribed to a difference in sources, because biomass-burning emission is an important source of airborne sulfate (Andreae et al., 1990) and more abundant in the non-urban region. In addition, an enhanced wet scavenging of sulfate due to more significant fog and cloud formation over Mt. Hua may also be responsible for such a non-correlation.

3.2. Back-trajectories analysis

Backward trajectories showed that wintertime air masses over the mountaintop are largely transported from the south and north directions, therefore, the total samples can be classified as two categories: (1) northerly and northwesterly and (2) southerly (Fig. 4). As shown in Table 4, galactosan, mannosan and levoglucosan presented a higher concentration in particles transported from southerly air masses than in those from the northerly, indicating that biofuel combustion is more significant in southern China. As mentioned above, sucrose and trehalose are metabolism products of biota in soil, thus both are more abundant in aerosols transported from the northerly air masses due to more airborne dust in north China (Table 4). Concentrations (69 ± 43 ng m^{-3}, Table 4) of plant wax derived n-alkanes in the northerly samples are similar to
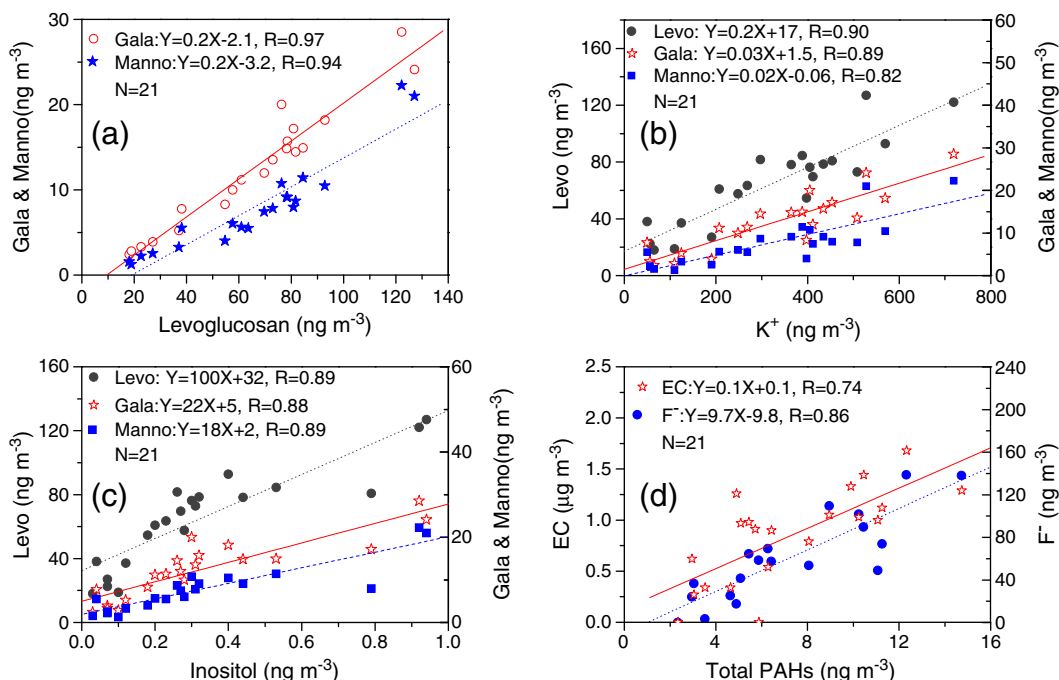
Fig. 3. Liner correlations between the measured species: (a) galactosan and mannosan vs levoglucosan (the typical biomass burning tracers); (b) organic tracers vs inorganic tracer (K^+) of biomass burning; (c) organic tracers of biomass burning vs inositol; (d) inorganic tracers (EC and F^-) vs organic tracers (total PAHs) of fossil fuel combustion.

those (75 ± 3.2 ng m^{-3}) in the southerly. However, fossil fuel derived n-alkanes (82 ± 11 ng m^{-3}) in the southerly samples are more abundant than in the northerly ones (49 ± 24 ng m^{-3}), together with a lower value of CPI (carbon preference index, odd-to-even, 2.8 ± 0.3 for the southerly and 3.6 ± 0.9 for the northerly), further suggesting more significant pollution due to fossil fuel combustion in southern China, which is consistent with our previous reported results on SO_4^{2-} and NO_3^- (Li et al., 2011). Coal burning emission is the major source of PAHs in the country as mentioned above, therefore, similar ratios of IP/BghiP (2.6 ± 0.4 for the northerly versus 2.9 ± 0.1 for the southerly, thereinafter) and BghiP/BeP (0.35 ± 0.06 versus 0.34 ± 0.01) were observed for the southerly and northerly samples.

3.3. Size distribution of sugars, n-alkanes and PAHs

3.3.1. Sugars

Table 5 shows the concentrations and geometric mean diameters (GMD) of sugars, n-alkanes and PAHs in fine

Table 3
Correlation coefficients (R) of sugars in PM$_{10}$ (N = 21).

	Arabitol	Fructose	Glucose	Mannitol	Sucrose	Trehalose
Arabitol	1					
Fructose	0.85	1				
Glucose	0.85	0.99	1			
Mannitol	0.95	0.95	0.94	1		
Sucrose	0.45	0.45	0.46	0.49	1	
Trehalose	0.91	0.88	0.88	0.94	0.60	1

(<2.1 µm) and coarse (>2.1 µm) modes, while Fig. 5 plots their detailed distributions in each size range.

Levoglucosan, galactosan and mannosan presented a unimodal size distribution, peaking at the size of 0.7–1.1 µm (Fig. 5a). A similar pattern was also found for inositol and K^+ (Li et al., 2011), again confirming those species are derived from biomass burning emissions. Such a unimodal distribution was also obtained in Baoji, a city near Mt. Hua (Wang et al., 2011a), and Nanjing, a city located in east coastal China (Wang et al., 2009d). Being different from the dehydrated sugars, non-dehydrated sugars like glucose and mannitol are characterized by a bimodal distribution pattern with two equivalent peaks at the ranges of 1.1–2.1 µm and 5.8–9.0 µm, respectively (Fig. 5b). Coarse mode of these compounds is generally produced via mechanical processes such as wind abrasion with plant surface and resuspension of soil, while fine mode of these sugars is derived from uncombusted biomass materials. For example, Wang et al. (2011b) found that glycerol, a reduced sugar, is enriched in fresh smoke particles of wheat straw burning with a minor amount of glucose and mannitol and mostly stay in particles with a diameter less than 2 µm.

3.3.2. n-Alkanes
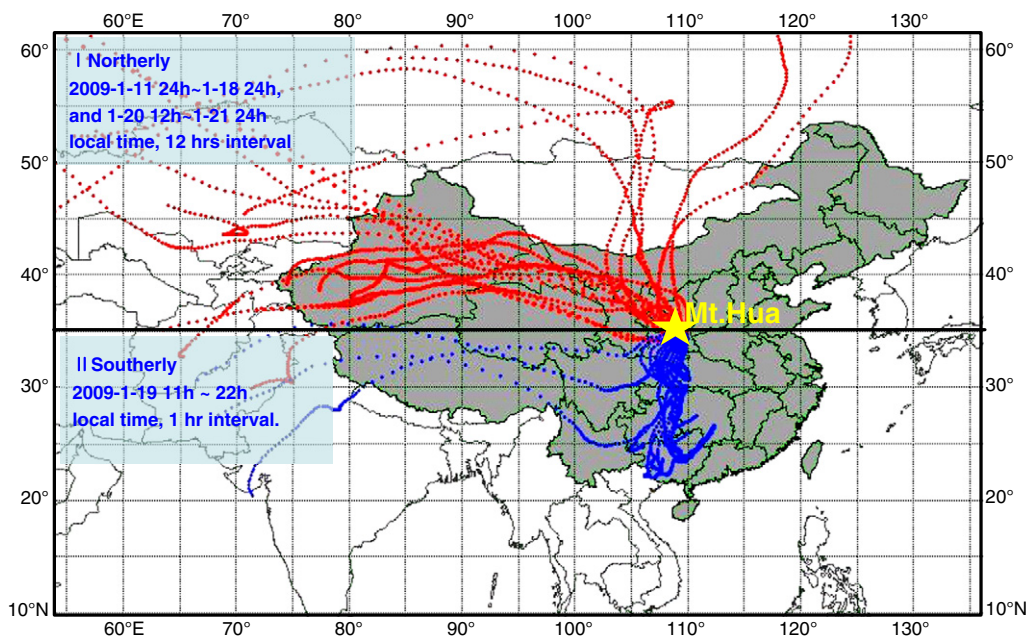
As shown in Table 5, both fossil fuel derived (35 ± 11 ng m^{-3}) and plant wax derived n-alkanes (48 ± 24 ng m^{-3}) are enriched in fine mode, being 4 and 2 times more than those in coarse mode, respectively. Simoneit et al. (2004b) has reported that n-alkanes originated from plant wax presents an odd number preference, in contrast to those derived from fossil fuel combustion, which have no odd/even carbon number preference. Thus, carbon preference index

Fig. 4. Backward air mass trajectories passing over Mt. Hua (34°29′ N, 110°05′E, and the altitude were set as 2070 m above the mean sea level) in winter (I. Jan. 11–18, and 20–21, 12 h interval; II. Jan. 19 and 22, 1 h interval).

(CPI, odd/even) of n-alkanes has been employed to recognize the contributions from different sources, as it is nearly unity and >5 for fossil fuel derived and plant wax derived n-alkanes, respectively (Simoneit et al., 2004b; Mazquiarán and de Pinedo, 2007). Carbon preference index (CPI, odd-to-even) in the coarse mode is 5.9 ± 1.5 and much higher than that (3.5 ± 0.5) in fine mode, indicating that n-alkanes in coarse particles are of biogenic origins. GMD of plant wax derived n-

Table 4
Concentrations (ng m^{-3}) and diagnostic ratios of sugars, n-alkanes and PAHs in PM$_{10}$ from northerly and southerly air masses.

	Northerly (N = 19)	Southerly (N = 2)	S/N ratio[a]
I. Sugars			
Galactosan	11 ± 5.4	26 ± 2.2	2.4
Mannosan	6.3 ± 3.1	22 ± 0.6	3.4
Levoglucosan	59 ± 24	125 ± 2.5	2.1
Sucrose	2.9 ± 2.7	1.9 ± 0.10	0.70
Trehalose	2.6 ± 2.3	1.8 ± 0.39	0.67
II. n-alkanes			
Total n-alkanes	118 ± 65	157 ± 7.6	1.3
Plant wax	69 ± 43	75 ± 3.2	1.1
Fossil fuel	49 ± 24	82 ± 11	1.7
CPI[b]	3.6 ± 0.9	2.8 ± 0.31	
III. PAHs			
Total PAHs	7.3 ± 3.5	7.8 ± 2.1	1.1
IP/BghiP	2.6 ± 0.4	2.9 ± 0.10	
BghiP/BeP	0.35 ± 0.06	0.34 ± 0.01	
BaP/BeP	0.48 ± 0.10	0.51 ± 0.05	
PM$_{10}$ (μg m^{-3})	52 ± 27	67 ± 4.3	1.3
OC (μg m^{-3})	5.6 ± 2.3	9.6 ± 0.6	1.7
EC (μg m^{-3})	0.8 ± 0.5	1.1 ± 0.2	1.4

[a] Ratios of mean concentrations from southerly to northerly.
[b] CPI, carbon prefence index for n-alkanes: $(C_{19} + C_{21} + C_{23} + C_{25} + C_{27} + C_{29} + C_{31} + C_{33} + C_{35})/(C_{18} + C_{20} + C_{22} + C_{24} + C_{26} + C_{28} + C_{30} + C_{32} + C_{34})$.

alkanes are 1.12 ± 0.03 μm and 7.75 ± 3.21 μm in fine and coarse modes, respectively, larger than those originated from fossil fuel (0.89 ± 0.06 μm in fine mode and 6.40 ± 2.15 μm in coarse mode, respectively, Table 5).

As can be seen in Fig. 5c, concentrations of plant wax derived n-alkanes in particles less than 1.1 μm are similar to those of fossil fuel derived n-alkanes but more abundant than fossil fuel derived n-alkanes in particles larger than 1.1 μm. CPI values of n-alkanes in particles larger than 2.1 μm ranged from 3.9 to 7.9 (Fig. 5e), further revealing that n-alkanes in coarse particles are mostly originated from natural sources. In contrast, CPI values in particles less than 2.1 μm decrease as a decrease in particle size with the smallest (CPI = 1.7) found for the backup stage (particle with a diameter<0.4 μm) (Fig.5e), indicating that fossil fuel derived n-alkanes are preferentially enriched in submicrometer particles.

3.3.3. PAHs

PAHs are 7.9 ± 1.3 ng m^{-3} in fine mode and 0.8 ± 0.4 ng m^{-3} in coarse mode (Table 5). HMW BbkF and IP are the dominant species in fine mode, whereas the most abundant PAHs in coarse mode are LMW ones (e.g., Phe and Flu). As shown in Fig. 5d, both LMW (i.e., 3,4-ring) and HMW (i.e., 5,6-ring) PAHs displayed a unimodal pattern, maximizing at the size of 0.7–1.1 μm. Concentration ratios of 3,4- ring PAHs to 5,6- ring PAHs are 0.8–1.0 in fine mode and 1.5–3.9 in coarse mode (Fig. 5f). LMW PAHs (i.e., 3,4-ring PAHs) in solid phase can evaporate into the air and subsequently adsorb/condense onto pre-existing particles due to their volatile nature (Birgul et al., 2011; Offenberg and Baker, 1999). Thus Phe and Flu move toward larger particles faster than HMW PAHs (e.g., 5,6- ring PAHs), resulting in relatively more abundant Phe and Flu in coarse mode (Fig. 5f). GMD of PAHs is 0.90 ± 0.02 μm in fine mode, which is very close to

Table 5
Concentrations (ng m^{-3}), and geometric mean diameters (GMD, μm) of sugars, n-alkanes and PAHs in fine and coarse particles from Mt. Hua during winter.

N = 3	Fine (<2.1 μm)		Coarse (>2.1 μm)	
	Concentration	GMD[a]	Concentration	GMD[a]
I. Sugars				
Galactosan (Gala)	8.3 ± 1.8	0.95 ± 0.03	2.1 ± 1.1	4.71 ± 1.35
Mannosan (Manno)	5.5 ± 1.4	0.90 ± 0.04	1.1 ± 0.5	4.81 ± 1.47
Levoglucosan (Levo)	64 ± 14	0.87 ± 0.03	12 ± 5.8	4.41 ± 1.18
Arabitol (Arab)	0.6 ± 0.2	0.87 ± 0.06	2.0 ± 0.6	10.66 ± 1.19
Fructose (Fluc)	1.4 ± 0.7	0.85 ± 0.07	2.3 ± 1.1	14.55 ± 0.89
Glucose (Gluc)	2.8 ± 1.9	0.94 ± 0.19	2.6 ± 1.2	14.36 ± 1.18
Mannitol (Manni)	0.6 ± 0.6	0.98 ± 0.24	1.3 ± 0.3	10.68 ± 1.31
Inositol (Inos)	0.2 ± 0.1	0.83 ± 0.02	0.1 ± 0.0	11.21 ± 3.77
Sucrose (Sucr)	0.3 ± 0.2	0.85 ± 0.04	0.9 ± 0.4	14.88 ± 1.76
Trehalose (Treh)	0.2 ± 0.1	1.06 ± 0.06	1.2 ± 0.6	10.24 ± 1.8
Subtotal	84 ± 19	0.88 ± 0.04	26 ± 11	6.71 ± 1.33
II. n-alkanes				
Octadecane (C$_{18}$)	1.0 ± 0.28	0.76 ± 0.06	0.8 ± 0.4	7.22 ± 1.11
Nonadecane (C$_{19}$)	0.7 ± 0.1	0.57 ± 0.03	0.3 ± 0.2	8.13 ± 2.03
Icosane (C$_{20}$)	0.8 ± 0.2	0.64 ± 0.03	0.3 ± 0.1	6.45 ± 1.47
Henicosane (C$_{21}$)	1.6 ± 0.5	0.76 ± 0.05	0.3 ± 0.2	6.14 ± 1.78
Docosane (C$_{22}$)	2.0 ± 0.7	0.84 ± 0.04	0.3 ± 0.2	5.62 ± 1.67
Tricosane (C$_{23}$)	3.2 ± 1.1	0.89 ± 0.04	0.5 ± 0.3	6.00 ± 2.40
Tetracosane (C$_{24}$)	2.7 ± 0.9	0.87 ± 0.04	0.4 ± 0.2	5.67 ± 1.95
Pentacosane (C$_{25}$)	4.4 ± 1.5	0.92 ± 0.06	0.8 ± 0.5	6.42 ± 2.93
Hexacosane (C$_{26}$)	2.8 ± 0.9	0.89 ± 0.07	0.5 ± 0.3	5.97 ± 2.37
Heptacosane (C$_{27}$)	6.2 ± 2.4	0.99 ± 0.07	1.7 ± 1.2	6.55 ± 3.04
Octacosane (C$_{28}$)	2.7 ± 0.9	0.93 ± 0.08	0.6 ± 0.4	6.11 ± 2.14
Nonacosane (C$_{29}$)	22 ± 10	1.10 ± 0.03	9.5 ± 7.2	6.82 ± 2.76
Triacotane (C$_{30}$)	2.8 ± 0.9	0.95 ± 0.08	0.7 ± 0.4	6.51 ± 2.34
Hentriacotane (C$_{31}$)	20 ± 10	1.13 ± 0.03	12 ± 9.2	8.31 ± 3.32
Dotriacotane (C$_{32}$)	2.1 ± 0.7	0.97 ± 0.08	0.5 ± 0.2	6.71 ± 2.80
Tritriacotane (C$_{33}$)	5.8 ± 2.6	1.08 ± 0.04	2.3 ± 1.6	9.18 ± 3.85
Tetratriacotane (C$_{34}$)	1.2 ± 0.4	0.99 ± 0.04	0.3 ± 0.2	7.03 ± 2.33
Pentatriacotane (C$_{35}$)	2.1 ± 0.9	1.00 ± 0.14	0.6 ± 0.3	7.15 ± 2.73
Subtotal	84 ± 35	1.01 ± 0.05	32 ± 23	7.36 ± 2.89
Plant wax n-alkanes[b]	48 ± 24	1.12 ± 0.03	24 ± 19	7.75 ± 3.21
Fossil fuel n-alkanes[b]	35 ± 11	0.89 ± 0.06	8.2 ± 4.4	6.40 ± 2.15
III. PAHs				
Phenanthrene (Phe)	0.76 ± 0.24	0.93 ± 0.03	0.17 ± 0.07	6.31 ± 1.6
Anthracene (Ant)	0.08 ± 0.02	0.87 ± 0.02	0.03 ± 0.01	6.86 ± 1.06
Fluoranthene (Flu)	0.89 ± 0.22	0.93 ± 0.03	0.14 ± 0.07	5.46 ± 1.48
Pyrene (Pyr)	0.61 ± 0.12	0.91 ± 0.02	0.07 ± 0.04	5.66 ± 1.65
216 PAH isomers	0.4 ± 0.1	0.88 ± 0.02	nd	nd
Benz(a)anthracene (BaA)	0.2 ± 0.01	0.91 ± 0.01	nd	nd
Chrysene/Triphenylene (CT)	0.7 ± 0.14	0.93 ± 0.01	0.06 ± 0.03	5.77 ± 2.28
Benzo(b/k)fluoranthene (BbkF)	1.21 ± 0.19	0.89 ± 0.02	0.12 ± 0.07	6.84 ± 1.03
Benzo(e)pyrene (BeP)	1.0 ± 0.2	0.9 ± 0.01	0.1 ± 0.0	5.66 ± 1.65
Benzo(a)pyrene (BaP)	0.46 ± 0.04	0.91 ± 0.02	nd	nd
Perylene (Per)	0.1 ± 0.0	0.91 ± 0.05	nd	nd
Indeno[123-cd]pyrene (IP)	0.92 ± 0.12	0.89 ± 0.03	0.05 ± 0.04	5.32 ± 1.97
Dibenz(a,h)anthracene (DBA)	0.18 ± 0.05	0.85 ± 0.14	0.05 ± 0.05	11.9 ± 1.46
Benzo(ghi)perylene (BghiP)	0.34 ± 0.04	0.86 ± 0.04	0.04 ± 0.03	8.84 ± 1.31
Subtotal	7.9 ± 1.3	0.90 ± 0.02	0.8 ± 0.4	6.44 ± 1.35

[a] logGMD = (ΣC$_i$ log Dp$_i$)/ ΣC$_i$, where C$_i$ is the concentration of compound in size i and Dp$_i$ is the geometric mean particle diameter collected on stage i (Hinds, 1999).
[b] Plant wax n-alkanes: calculated as the excess odd homologues-adjacent even homologues average and the difference from the total nalkanes is the fossil fuel-derived amount (Simoneit et al., 1991, 2004b).

the value (0.89 ± 0.06 μm, Table 5) of fossil fuel derived n-alkanes, suggesting a common source of fossil fuel combustion. Compared to those in Chinese urban areas like Baoji (Wang et al., 2009a) and Nanjing (Wang et al., 2009d), GMDs of PAHs in fine mode at Mt. Hua is about 8–20% larger. This is probably caused by a difference in sources, because PAHs in the urban areas are mostly derived from fossil fuel combustion, which are of smaller sizes, whereas the mountain PAHs are in part derived from rural biofuel burning, which are of larger sizes (Wang et al., 2009d). Furthermore, we found that the fine mode GMDs of PAHs at Mt. Hua is smaller than those (0.99 ± 0.11 μm) observed at Mt. Tai in North China Plain during winter (Wang et al., 2009a), which can be ascribed to the more significant biomass burning emission in the Mt. Tai region (Wang et al., 2011a), contributing more large size of PAH aerosols.
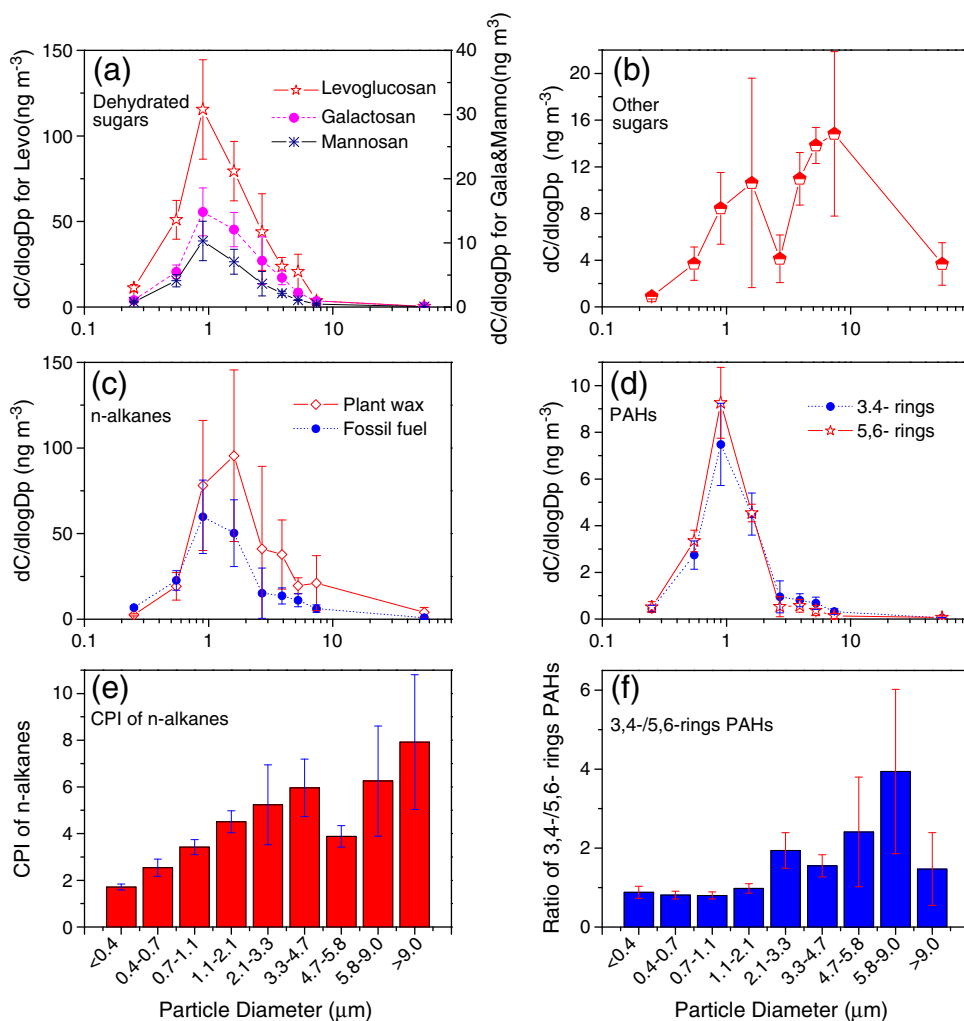
Fig. 5. Size distributions for concentrations and diagnostic ratios of sugars, *n*-alkanes and PAHs in the Mt. Hua atmosphere in winter.

3.4. Principal component analysis (PCA) for sources

To further investigate the possible sources of the mountain aerosols, PCA was used in this study. A total of 11 tracers were selected from the current data set and our previous study (Li et al., 2011). As shown in Table 6, factor 1 presents

high loadings with C_{29} and C_{31} *n*-alkanes, representing a source of plant wax emission (Simoneit et al., 2004b). Levoglucosan and K^+, both are tracers of biomass burning smoke (Mariano et al., 2010; Simoneit et al., 2004a; Watson et al., 2001; Zdrahal et al., 2002), also show a high loading for Factor 1. Thus this factor can be considered as a source

Table 6
Principal component analysis for selected components of PM$_{10}$ samples.

N = 21	Factor 1	Factor 2	Factor 3	Factor 4
K^+	0.59	0.48	0.37	0.51
Mg^{2+}	0.13	0.33	0.90	0.21
Ca^{2+}	0.22	0.17	0.93	0.20
F^-	0.43	0.85	0.22	0.07
Nonacosane(C_{29})	0.93	0.26	0.15	0.19
Hentriacotane (C_{31})	0.94	0.20	0.17	0.16
PAHs	0.14	0.90	0.27	0.22
Levoglucosan	0.78	0.21	0.19	0.47
NO_3^-	0.58	0.55	0.27	0.45
SO_4^{2-}	0.34	0.14	0.51	0.77
NH_4^+	0.63	0.36	0.18	0.65
% of Variance	34	23	22	17
Source	Biofuel combustion plus plant emission	Fossil fuel combustion	Soil and dust emission	Long-range transport

Table 7

Comparison of concentrations (ng m^{-3}) and compositions of sugars, *n*-alkanes and PAHs at Mt. Hua with those from other East Asia mountain, marine and urban regions and the free troposphere.

	Mountain sites		Free troposphere (aircraft)		Marine sites		Lowland urban sites							
	Mt. Hua, China[a]	Mt. Tai, China[b]	East coastal China[c]	Sea of Japan[d]	Gosan, Korea[e]	Chichi-Jima, Japan[f]	SE China[g]	NE China[g]	Central China[g]	N/NW China[g]	Baoji, China[h]	Hong Kong, China[i]	Gwangju, Korea[j]	Tokyo, Japan[k]
	Winter 2009	Winter	Winter 2003	Spring 2001	Spring 2005	Annual 1990–1993	Winter 2003	Winter 2003	Winter 2003	Winter 2003	Winter 2008	Winter 1993	Spring 2001	Winter 1997
	PM$_{10}$	PM$_9$	PM$_{2.5}$	TSP	TSP	TSP	PM$_{2.5}$	PM$_{2.5}$	PM$_{2.5}$	PM$_{2.5}$	PM$_{10}$	TSP	PM$_{2.5}$	TSP
I. Sugars														
Levo.	65	na	38	4	36	na	401	213	2955	115	901	na	18	na
Fruc.	5.4	na	17	8.5	14	na	28	3	4	na	73	na	na	na
Gluc.	5.5	na	35	na	15	na	13	6	35	2	55	na	na	na
Sucr.	2.8	na	16	0.9	52	na	5	5	4	1	219	na	na	na
M/G[l]	0.66	na	na	na	na	na	na	na	na	na	0.55	na	na	na
II. n-Alkanes														
Total	121	126	157	20	32	2	434	370	1191	529	1733	184	37	na
CPI[m]	3.5	1.3	1.1	1.3	2.3	4.5	1.2	1.1	1.3	1.1	1.3	1.3	0.9	na
III. PAHs														
Total	7.3	58	24	na	5	na	101	153	628	201	594	17	16	36
IP/BghiP[n]	2.7	1.9	1.2	na	1.2	na	1.1	1.3	1.2	1.2	1.1	0.65	0.61	0.76
BghiP/BeP[n]	0.35	0.8	1.3	na	0.89	Na	1.3	1.2	1.2	1.1	1.1	1.6	1.5	na
BaP/BeP	0.48	0.67	0.8	na	0.65	Na	0.72	1.0	1.0	0.87	0.79	0.47	0.85	na

[a] This study. 2060 m a.s.l.
[b] Wang et al., 2009a. 1534 m a.s.l.
[c] Wang et al., 2007. 500–3000 m, a.s.l.
[d] Simoneit et al., 2004c. 29–4034 m a.s.l.
[e] Wang et al., 2009c.
[f] Kawamura et al., 2003.
[g] Wang et al., 2006 (SE China: Shanghai, Guangzhou, Wuhan, Xiamen, and Hangzhou; NE China: Beijing, Tianjin, Qingdao and Changchun; Central China: Xi'an and Chongqing; NW China: Yulin and Jinchang).
[h] Xie et al., 2009, 2010.
[i] Zheng et al., 1997.
[j] Park et al., 2006.
[k] Tang et al., 2005.
[l] M/G: the mean ratio of mannosan/galactosan(M/G value in differ sources: grass:0.23, Oros et al., 2006; deciduous tree: 0.52, Oros and Simoneit, 2001b; conifer: 0.94, Oros and Simoneit, 2001a).
[m] CPI, carbon preference index, CPI = ΣOdd /ΣEven *n*-alkanes (Simoneit et al., 2004b).
[n] IP/BghiP in different sources is 0.2 for gasoline exhaust, 0.5 for diesel exhaust and 1.3 for coal emission (Grimmer et al., 1981), while Bghip/BeP in different sources is 2.0 for vehicle exhaust and 0.8 for coal emission (Ohura et al., 2004).

of biomass burning plus plant emission. Factor 2 is dominated by F^- and PAHs, and representative of fossil fuel combustion. Factor 3 well correlates with crustal matters (e.g., Ca^{2+} and Mg^{2+}), therefore, is indicative of soil and dust emission. Since factor 4 shows strong correlation with sulfate and ammonium and a relatively weaker correlation with K^+, PAHs and levoglucosan, here we think it represents a long-range transport. As seen in Table 6, biofuel combustion plus plant emission is the most important source of the mountain aerosols, accounting for 34% of the total variance, followed by fossil fuel combustion, soil and dust emission and long-range transport, explaining 23%, 22% and 17% of the variance, respectively.

3.5. Comparison with data from other urban, mountain, marine and aircraft observations

To obtain a panorama of organic aerosols over East Asia, here we compare the compositions of sugars, *n*-alkanes and PAHs at Mt. Hua with those data acquired from other urban, mountain, marine and aircraft measurements conducted in East Asia (see Table 7). Levoglucosan is detectable at all sites with a range from 4 ng m^{-3} in Japan Sea to 2955 ng m^{-3} in central China, indicating an ubiquity of biomass burning emission in this region. Levoglucosan is abundant in all Chinese cities (115–2955 ng m^{-3}), suggesting that pollution caused by biomass burning in the country cannot be neglected since much effort has been concentrated in reducing emissions from coal combustion. Mean ratio of mannosan to galactosan (M/G) in the Mt. Hua PM$_{10}$ samples was 0.66, indicating that more deciduous trees (M/G = 0.52, Oros and Simoneit, 2001b) rather than conifer trees (0.94, Oros and Simoneit, 2001a) and grass (0.23, Oros et al., 2006) are burned for cooking and heating in Guanzhong Plain, which is consist with the previous study at Baoji (M/G = 0.55) (Xie et al., 2010), a middle scale city near Mt. Hua. Sugars derived from soil microorganisms (e.g. fructose, glucose and sucrose) are 0.9–219 ng m^{-3} at all the sites, indicating that wintertime dust emission in East Asia is also significant.

Concentrations of *n*-alkanes in Chinese inland cities are 4–40 times higher than other developed cities (e.g., Hong Kong, China, Gwangju, South Korea and Tokyo, Japan, Table 7) with CPI close to unity, demonstrating a high level of anthropogenic pollution in these developing areas. *n*-Alkanes at Mt. Hua (121 ng m^{-3}, Table 7) and Mt. Tai (126 ng m^{-3}) are similar to those (157 ng m^{-3}) measured over east coastal China by aircraft, revealing a homogeneous distribution in the free troposphere from the central to the east coastal. However, compared to the CPI (3.5, Table 7) of *n*-alkanes at Mt. Hua, the much lower CPI (1.3 at Mt. Tai and 1.1 over east coastal China, Table 7) in the free troposphere over the east coastal region indicates more significant pollution from fossil fuel emissions. CPI of *n*-alkanes in all the cities are in the range of 0.9–1.3, revealing a predominance of fossil fuel emission in urban area of East Asia. In general, *n*-alkanes with a CPI more than 5 are considered as plant wax (Simoneit et al., 2004b; Mazquiarán and de Pinedo, 2007), thus the CPI values of 2.3 (Table 7) at Jeju Island, Korea and 4.5 (Table 7) at Chichi-jima Japan may suggest that primary organic pollutants emitted from fossil fuel combustion are abundant in marine region near the Asia continent but almost disappear in remote marine area.

Similar to *n*-alkanes, concentrations of PAHs are much higher in Chinese inland cities than in other urban areas. Moreover, PAHs at Mt. Tai are nearly one order of magnitude higher than those at Mt. Hua, again confirming an enhanced anthropogenic pollution in east China, which is consistent with satellite observations (Wittrock et al., 2006; van Donkelaar et al., 2010). Grimmer et al. (1981) reported that diagnostic ratios of IP/BghiP are 0.2, 0.5, and 1.3 in the smokes from gasoline, diesel, and coal combustions, respectively. Ohura et al. (2004) further reported that BghiP/BeP is 2.0 and 0.8 in emissions from vehicle exhaust and coal burning. These ratios are cited here to investigate PAH sources. IP/BghiP ratios are 1.1–1.3 in Chinese cities and 2.7 at Mt. Hua, which suggests that coal-burning emission is the major source especially in inland China. In contrast, IP/BghiP ratios in Hong Kong (China), Gwangju (Korea) and Tokyo (Japan) are 0.65, 0.61 and 0.76, respectively, which indicates that vehicle exhaust is the major source. Same results can also be obtained by comparing the BghiP/BeP ratios. Such a spatial distribution pattern of PAH compositions over East Asia further confirmed our previous conclusion that PAHs in China are mostly derived from coal combustion while those in other developed countries are largely originated from vehicle exhausts (Wang et al., 2006, 2007, 2009a, 2009c).

BaP is labile to photochemical degradation while its isomer BeP is much stable, thus the ratio of BaP/BeP can be thought as an indicator of aerosol ageing (Wang et al., 2009c; Xie et al., 2009). As shown in Table 7, BaP/BeP in Hong Kong is the lowest among all Chinese urban sites, suggesting aerosols are more aged in Hong Kong. In inland China, BaP/BeP increased from 0.72 in the southeast cities to 1.0 in the northeast cities, suggesting that photochemical degradation of aerosols is stronger in southern China than in northern China, most likely due to a difference in wintertime temperature. Furthermore, the ratio showed an increasing trend with a decrease in altitude, ranging from 0.48 at Mt. Hua (2060 m, a.s.l.), 0.67 at Mt. Tai (1545 m, a.s.l.) to 1.0 in central Chinese cities (<500 m, a.s.l.), suggesting an enhanced photochemical oxidation in the free troposphere.

4. Summary and Conclusion

Wintertime PM$_{10}$ and size-resolved samples in Mt. Hua, central China were determined for sugars, *n*-alkanes and PAHs on a molecular level. Levoglucosan (65 ± 30 ng m^{-3}) in PM$_{10}$ samples was the most abundant species among the sugar class, followed by galactosan (12 ± 6.8 ng m^{-3}) and mannosan (7.8 ± 5.4 ng m^{-3}). *n*-Alkanes in PM$_{10}$ was 121 ± 63 ng m^{-3} with C$_{31}$ (32 ± 18 ng m^{-3}) and C$_{29}$ (30 ± 18 ng m^{-3}) being the most abundant congeners, and characterized by a CPI of 3.5 with about 40% of the total from fossil fuel combustions. PAHs in the samples was 7.3 ± 3.4 ng m^{-3} with Flu (1.1 ± 0.4 ng m^{-3}) and BbkF (0.9 ± 0.5 ng m^{-3}) being the highest species. These organics are 1–2 orders of magnitude lower than those in urban areas in central China. Levoglucosan and fossil fuel derived *n*-alkanes are more abundant in the air masses from southern China than in those from northern China, although such a spatial difference was not found for PAHs, suggesting that emissions from biomass burning and

vehicle exhausts are more significant in southern part of the country. Size distributions showed that combustion derived organics such as dehydrated sugars, fossil fuel *n*-alkanes and PAHs presented a unimodal pattern, peaking at 0.7–1.1 μm, while non-dehydrated sugars (e.g., glucose, mannitol and sucrose) and plant wax derived *n*-alkanes displayed a bimodal pattern, peaking at 0.7–2.1 and 5.8–9.0 μm ranges.

PCA analysis indicates that biomass burning plus plant emission is the major source of wintertime airborne particles at Mt. Hua, followed by fossil fuel combustion, soil and dust emission and long-range transport, which is different from the cases in inland urban areas where fossil fuel combustion is the most important source. Molecular compositions demonstrate that coal burning is still the major source of PAHs in the country, although vehicle number has sharply increased recently. Diagnostic ratios of PAHs further indicate that photo-oxidation of aerosols was more significant in the troposphere of Mt. Hua and Mt. Tai compared to those in lowland urban areas.

Acknowledgements

References

Andreae, M.O., Talbot, R.W., Berresheim, H., Beecher, K.M., 1990. Pricipitation chemistry in central Amazonia. J. Geophys. Res. Atmos. 95, 16987–16999.

Birgul, A., Tasdemir, Y., Cindoruk, S.S., 2011. Atmospheric wet and dry deposition of polycyclic aromatic hydrocarbons (PAHs) determined using a modified sampler. Atmos. Res. 101, 341–353.

Engling, G., Lee, J.J., Tsai, Y.W., Lung, S.C.C., Chou, C.C.K., Chan, C.Y., 2009. Size-resolved anhydrosugar composition in smoke aerosol from controlled field burning of rice straw. Aerosol Sci. Technol. 43, 662–672.

Gaga, E.O., Ari, A., 2011. Gas-particle partitioning of polycyclic aromatic hydrocarbons (PAHs) in an urban traffic site in Eskisehir, Turkey. Atmos. Res. 99, 207–216.

Grimmer, G., Jacob, J., Naujack, K.W., Dettbarn, G., 1981. Profile of the polycyclic aromatic hydrocarbons from used engine oil — inventory by GC GC/MS — PAH in environmental materials, Part 2. Fresenius Z. Anal. Chem. 309, 13–19.

Hanedar, A., Alp, K., Kaynak, B., Baek, J., Avsar, E., Odman, M.T., 2011. Concentrations and sources of PAHs at three stations in Istanbul, Turkey. Atmos. Res. 99, 391–399.

Hinds, W.C., 1999. Aerosol Technology: Properties, Behavior, and Measurement of Airborne Particles. John Wiley and Sons, New York.

Huebert, B.J., Bates, T., Russell, P.B., Shi, G.Y., Kim, Y.J., Kawamura, K., Carmichael, G., Nakajima, T., 2003. An overview of ACE-Asia: Strategies for quantifying the relationships between Asian aerosols and their climatic impacts. J. Geophys. Res.-Atmos. 108, D23. doi:10.1029/2003jd003550.

Kawamura, K., Ishimura, Y., Yamazaki, K., 2003. Four years' observations of terrestrial lipid class compounds in marine aerosols from the western North Pacific. Global Biogeochem. Cycles 17. doi:10.1029/2001GB001810.

Ladji, R., Yassaa, N., Balducci, C., Cecinato, A., Meklati, B.Y., 2009. Annual variation of particulate organic compounds in PM(10) in the urban atmosphere of Algiers. Atmos. Res. 92, 258–269.

Li, J.J., Wang, G.H., Zhou, B.H., Cheng, C.L., Cao, J.J., Shen, Z.X., An, Z.S., 2011. Chemical composition and size distribution of wintertime aerosols in the atmosphere of Mt. Hua in central China. Atmos. Environ. 45, 1251–1258.

Mariano, G.L., Lopes, F.J.S., Jorge, M., Landulfo, E., 2010. Assessment of biomass burnings activity with the synergy of sunphotometric and LIDAR measurements in Sao Paulo, Brazil. Atmos. Res. 98, 486–499.

Mazquiarán, M.A.B., de Pinedo, L.C.O., 2007. Organic composition of atmospheric urban aerosol: Variations and sources of aliphatic and polycyclic aromatic hydrocarbons. Atmos. Res. 85, 288–299.

McMurry, P.H., 2000. A review of atmospheric aerosol measurements. Atmos. Environ. 34, 1959–1999.

Medeiros, P.M., Conte, M.H., Weber, J.C., Simoneit, B.R.T., 2006. Sugars as source indicators of biogenic organic carbon in aerosols collected above the Howland Experimental Forest, Maine. Atmos. Environ. 40, 1694–1705.

Menon, S., Hansen, J., Nazarenko, L., Luo, Y., 2002. Climate effects of black carbon aerosols in China and India. Science 297, 2250–2253.

Offenberg, J.H., Baker, J.E., 1999. Aerosol size distributions of polycyclic aromatic hydrocarbons in urban and over water atmospheres. Environ. Sci. Technol. 33, 3324–3331.

Ohura, T., Amagai, T., Fusaya, M., Matsushita, H., 2004. Polycyclic aromatic hydrocarbons in indoor and outdoor environments and factors affecting their concentrations. Environ. Sci. Technol. 38, 77–83.

Oros, D.R., Simoneit, B.R.T., 2001a. Identification and emission factors of molecular tracers in organic aerosols from biomass burning Part 1. Temperate climate conifers. Appl. Geochem. 16, 1513–1544.

Oros, D.R., Simoneit, B.R.T., 2001b. Identification and emission factors of molecular tracers in organic aerosols from biomass burning Part 2. Deciduous trees. Appl. Geochem. 16, 1545–1565.

Oros, D.R., bin Abas, M.R., Omar, N., Rahman, N.A., Simoneit, B.R.T., 2006. Identification and emission factors of molecular tracers in organic aerosols from biomass burning: Part 3. Grasses. Appl. Geochem. 21, 919–940.

Park, S.S., Bae, M.S., Schauer, J.J., Kim, Y.J., Cho, S.Y., Kim, S.J., 2006. Molecular composition of PM2.5 organic aerosol measured at an urban site of Korea during the ACE-Asia campaign. Atmos. Environ. 40, 4182–4198.

Peters, J., Seifert, B., 1980. Losses of benzo(a)pyrene under the conditions of high-volume sampling. Atmos. Environ. 14, 117–119.

Pio, C.A., Legrand, M., Alves, C.A., Oliveira, T., Afonso, J., Caseiro, A., Puxbaum, H., Sanchez-Ochoa, A., Gelencser, A., 2008. Chemical composition of atmospheric aerosols during the 2003 summer intense forest fire period. Atmos. Environ. 42, 7530–7543.

Rogge, W.F., Hildemann, L.M., Mazurek, M.A., Cass, G.R., Simoneit, B.R.T., 1993. Sources of fine organic aerosol. 4. Particulate abrasion products from leaf surfaces of urban plants. Environ. Sci. Technol. 27, 2700–2711.

Rosenfeld, D., Dai, J., Yu, X., Yao, Z.Y., Xu, X.H., Yang, X., Du, C.L., 2007. Inverse relations between amounts of air pollution and orographic precipitation. Science 315, 1396–1398.

Shen, Z.X., Arimoto, R., Cao, J.J., Zhang, R.J., Li, X.X., Du, N., Okuda, T., Nakao, S., Tanaka, S., 2008. Seasonal variations and evidence for the effectiveness of pollution controls on water-soluble inorganic species in total suspended particulates and fine particulate matter from Xi'an, China. J. Air Waste Manage. Assoc. 58, 1560–1570.

Simoneit, B.R.T., Sheng, G.Y., Chen, X.J., Fu, J.M., Zhang, J., Xu, Y.P., 1991. Molecular marker study of extractable organic matter in aerosols from urban areas of China. Atmos. Environ. Part A 25, 2111–2129.

Simoneit, B.R.T., Schauer, J.J., Nolte, C.G., Oros, D.R., Elias, V.O., Fraser, M.P., Rogge, W.F., Cass, G.R., 1999. Levoglucosan, a tracer for cellulose in biomass burning and atmospheric particles. Atmos. Environ. 33, 173–182.

Simoneit, B.R.T., Elias, V.O., Kobayashi, M., Kawamura, K., Rushdi, A.I., Medeiros, P.M., Rogge, W.F., Didyk, B.M., 2004a. Sugars-Dominant water-soluble organic compounds in soils and characterization as tracers in atmospheric particulate matter. Environ. Sci. Technol. 38, 5939–5949.

Simoneit, B.R.T., Kobayashi, M., Mochida, M., Kawamura, K., Lee, M., Lim, H.J., Turpin, B.J., Komazaki, Y., 2004b. Composition and major sources of organic compounds of aerosol particulate matter sampled during the ACE-Asia campaign. J. Geophys. Res.-Atmos. 109, D19s10. doi:10.1029/2004jd004598.

Simoneit, B.R.T., Kobayashi, M., Mochida, M., Kawamura, K., Huebert, B.J., 2004c. Aerosol particles collected on aircraft flights over the northwestern Pacific region during the ACE-Asia campaign: Composition and major sources of the organic compounds. J. Geophys. Res.-Atmos. 109, D19. doi:10.1029/2004jd004565.

Tang, N., Hattori, T., Taga, R., Igarashi, K., Yang, X.Y., Tamura, K., Kakimoto, H., Mishukov, V.F., Toriba, A., Kizu, R., Hayakawa, K., 2005. Polycyclic aromatic hydrocarbons and nitropolycyclic aromatic hydrocarbons in urban air particulates and their relationship to emission sources in the Pan-Japan Sea countries. Atmos. Environ. 39, 5817–5826.

van Donkelaar, A., Martin, R.V., Brauer, M., Kahn, R., Levy, R., Verduzco, C., Villeneuve, P.J., 2010. Global estimates of ambient fine particulate matter concentrations from satellite-based aerosol optical depth: Development and application. Environ. Heal. Perspect. 118, 847–855.

Wang, G.H., Kawamura, K., Lee, S., Ho, K.F., Cao, J.J., 2006. Molecular, seasonal, and spatial distributions of organic aerosols from fourteen Chinese cities. Environ. Sci. Technol. 40, 4619–4625.

Wang, G.H., Kawamura, K., Hatakeyama, S., Takami, A., Li, H., Wang, W., 2007. Aircraft measurement of organic aerosols over China. Environ. Sci. Technol. 41, 3115–3120.

Wang, G., Kawamura, K., Xie, M., Hu, S., Gao, S., Cao, J., An, Z., Wang, Z., 2009a. Size-distributions of *n*-alkanes, PAHs and hopanes and their sources in

the urban, mountain and marine atmospheres over East Asia. Atmos. Chem. Phys. 9, 8869–8882.

Wang, G.H., Kawamura, K., Umemoto, N., Xie, M.J., Hu, S.Y., Wang, Z.F., 2009b. Water-soluble organic compounds in PM2.5 and size-segregated aerosols over Mount Tai in North China Plain. J. Geophys. Res.-Atmos. 114, D19208. doi:10.1029/2008jd011390.

Wang, G.H., Kawamura, K., Lee, M., 2009c. Comparison of organic compositions in dust storm and normal aerosol samples collected at Gosan, Jeju Island, during spring 2005. Atmos. Environ. 43, 219–227.

Wang, G.H., Kawamura, K., Xie, M.J., Hu, S.Y., Cao, J.J., An, Z.S., Waston, J.G., Chow, J.C., 2009d. Organic Molecular Compositions and Size Distributions of Chinese Summer and Autumn Aerosols from Nanjing: Characteristic Haze Event Caused by Wheat Straw Burning. Environ. Sci. Technol. 43, 6493–6499.

Wang, G., Xie, M., Hu, S., Gao, S., Tachibana, E., Kawamura, K., 2010. Dicarboxylic acids, metals and isotopic compositions of C and N in atmospheric aerosols from inland China: implications for dust and coal burning emission and secondary aerosol formation. Atmos. Chem. Phys. 10, 6087–6096.

Wang, G.H., Kawamura, K., Xie, M.J., Hu, S.Y., Li, J.J., Zhou, B.H., Cao, J.J., An, Z.S., 2011a. Selected water-soluble organic compounds found in sized-resolved aerosols collected from urban, mountain, and marine atmospheres over East Asia. Tellus B 63, 371–381.

Wang, G.H., Cheng, C.L., Li, J.J., Zhou, B.H., Xie, M.J., Hu, S.Y., Kawamura, K., Chen, Y., 2011b. Molecular composition and size distribution of sugars, sugar-alcohols and carboxylic acids in airborne particles during a severe urban haze event caused by wheat straw burning. Atmos. Environ. 45, 2473–2479.

Watson, J.G., Chow, J.C., Houck, J.E., 2001. PM2.5 chemical source profiles for vehicle exhaust, vegetative burning, geological material, and coal burning in Northwestern Colorado during 1995. Chemosphere 43, 1141–1151.

Wittrock, F., Richter, A., Oetjen, H., Burrows, J.P., Kanakidou, M., Myriokefalitakis, S., Volkamer, R., Beirle, S., Platt, U., Wagner, T., 2006. Simultaneous global observations of glyoxal and formaldehyde from space. Geophys. Res. Lett. 33, L16804. doi:10.1029/2006GL026310.

Xie, M.J., Wang, G.H., Hu, S.Y., Han, Q.Y., Xu, Y.J., Gao, Z.C., 2009. Aliphatic alkanes and polycyclic aromatic hydrocarbons in atmospheric PM10 aerosols from Baoji, China: Implications for coal burning. Atmos. Res. 93, 840–848.

Xie, M., Wang, G., Hu, S., Gao, S., Han, Q., Xu, Y., Feng, J., 2010. Polar organic and inorganic markers in PM_{10} aerosols from an inland city of China - seasonal trends and sources. Sci. Total. Environ. 408, 5452–5460.

Zdrahal, Z., Oliveira, J., Vermeylen, R., Claeys, M., Maenhaut, W., 2002. Improved method for quantifying levoglucosan and related monosaccharide anhydrides in atmospheric aerosols and application to samples from urban and tropical locations. Environ. Sci. Technol. 36, 747–753.

Zheng, M., Wan, T.S.M., Fang, M., Wang, F., 1997. Characterization of the non-volatile organic compounds in the aerosols of Hong Kong - Identification, abundance and origin. Atmos. Environ. 31, 227–237.